International Journal of Technology (2015) 2: 254-263
ISSN 2086-9614

ANALYSIS OF SUCTION PILES FOR MOORING FLOATING STRUCTURE FOUNDATIONS IN CLAY SOIL AT DEEPWATER LEVELS

Irfan Budiman[1], Iwan Soedigdo[2*], Widjojo A. Prakoso[2]

[1]*PT. Rekadaya, Jakarta, Indonesia*
[2]*Department of Civil Engineering, Faculty of Engineering, Universitas Indonesia, Kampus UI Depok 16424, Indonesia*

(Received: July 2014 / Revised: November 2014 / Accepted: April 2015)

ABSTRACT

Oil and gas exploration is increasingly moving to deepwater locations to meet the increasing energy demands. In this environment, floating structures with suction pile foundations are commonly used because their cost-effectiveness. Some studies have been conducted to examine the behavior of suction piles in clay soils, but the typical clay conditions considered are normally consolidated and lightly over-consolidated. In this paper, the behavior of suction piles in under-consolidated clays and under-consolidated, normally consolidated clays, as extracted from actual deepwater soil conditions. The evaluation was performed using geotechnical 3D finite element software Plaxis. Suction piles with two different aspect ratios (L/D = 2 and 6) were considered, and the focus was on the effect of load angles (0° to 90°) and the effects of pad-eye positions (0.5 L to 0.9 L). For short piles, the load angles had a relatively insignificant effect on the overall ultimate resistance, while for long piles, the angles affected the overall resistance considerably with a decrease in resistance up to approximately 50 percent. This different behavior could be explained from the observed pile deformation patterns. The pad-eye positions affected the pile resistances significantly as well with a decrease in the resistance factor up to about 30 percent. Nevertheless, it can be concluded that the overall behavior of suction piles in combined clay conditions is practically similar to that of piles in normally consolidated and over-consolidated clays.

Keywords: Clay soil; Load inclination; Pad-eye; Suction pile; Undrained shear strength

1. INTRODUCTION

Oil and gas exploration is increasingly moving to deepwater locations to meet increasing energy demands. In this environment, floating structures are commonly used because of their cost-effectiveness. A floating structure is maintained in position by a mooring system, connecting the bottom end of the structure to anchors embedded in the sea floor. Suction piles have become a common anchor type for a variety of mooring systems in the last two decades.

A suction pile is a steel or concrete cylindrical tube, with an open bottom and a closed top. The ratio of length (L) to diameter (D) of the tube or the so-called aspect ratio (L/D) is generally less than 10. The wall thickness (t) to diameter ratio (t/D) is also small, generally varying from 0.3% to 0.6%. The installation of a suction pile consists of two (2) steps: the tube initially penetrating into the seabed due to its own weight, and secondly, the tube being pushed to the required depth by applying an unbalanced pressure by pumping water out of the tube.

---

[*] Corresponding author's email: iwanrs@eng.ui.ac.id, Tel. +62-21-7270029, Fax. +62-21-7270028
Permalink/DOI: http://dx.doi.org/10.14716/ijtech.v6i2.374

Some studies (e.g., Andresen et al. 2008, Supachawarote 2006) have shown that the resistance of suction piles in clays is affected by some factors, including the aspect ratio (L/D), the effect of loading rate and cyclic loading, the load angle, the mooring line pad-eye position, as well as the surrounding gap formation and adhesion reduction on pile wall. These studies assumed that clays were either normally consolidated or lightly over-consolidated.

This study focuses on the effect of the aspect ratio, as well as the load angle and location, on the axial pullout and lateral ultimate resistances of suction piles. The clays are assumed as being either under-consolidated or under-consolidated to normally consolidated. The resistance is evaluated using the three-dimensional (3-D) finite element approach. The resistance is subsequently compared to the results of a simplified method.

2. RESISTANCE OF SUCTION PILES

The axial pullout and lateral capacities of suction piles need to be evaluated in the design process. In clays, the predominant failure mechanism is the reverse end-bearing failure mechanism, specifically in the transient load conditions. This mechanism is particularly true for suction piles with a sealed lid, in which the soil response would be maintained in an undrained condition. In addition, the axial pullout resistance would also be provided by the outer wall soil-pile adhesion. The vertical ultimate resistance is determined by using the following:

$$V_{ult} = (\alpha \cdot s_{u\text{-}average}) \cdot A_p + (N_C \cdot s_{u\text{-}tip}) \cdot A_{tip} \qquad (1)$$

in which α is interface adhesion factor, $s_{u\text{-}average}$ is along pile average undrained shear strength, A_p is pile perimeter area, N_C is reverse end-bearing resistance factor, $s_{u\text{-}tip}$ is undrained pile tip shear strength, and A_{tip} is tip cross-sectional area.

The upper bound solution for the horizontal resistance of suction piles has been proposed by Randolph and House (2002) by considering the following:

- Passive and active conical failure wedges at shallow depths.
- Plane strain flow below conical failure wedges
- Spherical rotational flow zone. The sphere center may move upward and subsequently eliminate the flow zone.

The horizontal ultimate resistance for simplicity is determined by using the following:

$$H_{ult} = (N_H \cdot s_{u\text{-}average}) \cdot (L \cdot D) \qquad (2)$$

in which N_H is horizontal resistance factor, $s_{u\text{-}average}$ is along the average undrained pile shear strength, L and D are suction pile length and diameter, respectively.

For a combination of axial pullout and lateral loads, Supachawarote (2006) has proposed an elliptical failure envelope based on finite element analysis results of suction piles in normally consolidated and lightly over-consolidated soil at the optimum pad-eye position:

$$(H / H_{ult})^{a} + (V / V_{ult})^{b} = 1 \qquad (3)$$

in which H is applied lateral load, H_{ult} is lateral ultimate resistance, V is axial pullout load, and V_{ult} is axial pullout ultimate resistance. It is noted that Equation 3 applies for the optimum pad-eye position and load angle. The parameters *a* and *b* are the geometric factors given as follows:

$$a = 0.5 + L/D \tag{4}$$

$$b = 4.5 - L/3D \tag{5}$$

in which L and D are suction pile length and diameter, respectively.

3. RESEARCH METHOD

The soil profile adopted and the numerical model used, as well as the cases considered, are discussed in this section. Furthermore, the results would be synthesized and discussed in the following section.

3.1. Soil Profile

The soil profile adopted for this study (Figure 1) was based on the soil investigation report of the Gehem and Ranggas blocks located in Makassar Strait (Dutt & Associates 2007). The soil profile was developed based on test results of soils sampled using jumbo piston cores from four (4) locations at sea depths from 1585 to 1805 m. It is assumed that the most critical condition is the undrained (short-term) condition with the undrained shear strength s_u as the primary parameter. For depths < 13 m, the clayey soils are in under-consolidated conditions, indicated by a low s_u increase rate; for depths > 13 m, the soils are in normally consolidated conditions with a higher s_u increase rate.

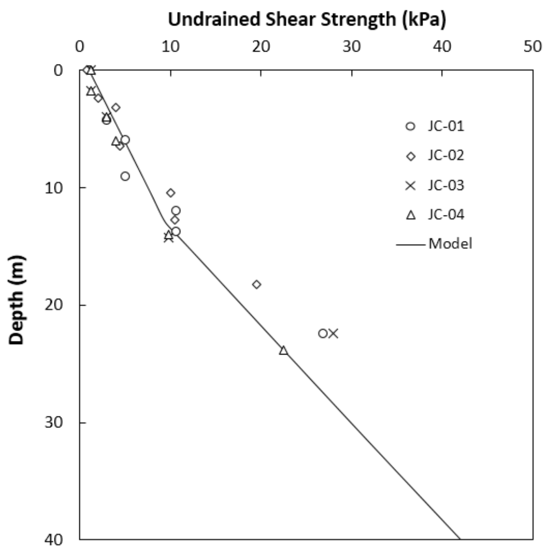

Figure 1 Undrained shear strength (data: Dutt and Associates 2007)

3.2. Finite Element Models

The resistance analysis was conducted using the finite element approach, and the software used was Plaxis 3D Foundation v2.1 (Plaxis BV 2008). Some basic assumptions about the soil behavior include undrained isotropic ($\phi = 0°$), independent of loading rate, elastic-perfectly plastic Mohr-Coulomb stress-strain relationship, and no gap forming between suction pile and soil. The suction pile is assumed to be a weightless rigid suction pile, and the soil plug inside the suction pile is assumed to be a stiff elastic material. Outer wall interface elements are used to model a slip between the pile and the soil, and the reduction factor for the interface elements is 0.65. All the parameters are summarized in Table 1.

Table 1 Material properties of undrained soil clay layer and interface

Parameter		Plaxis Input
Soil Unit Weight		13 kN/m^3
Poisson's Ratio		0.35
Young's Modulus:	Seabed	50 kN/m^2
	Increment (z < 13 m)	325 kN/m^2
	Increment (z > 13 m)	600 kN/m^2
Cohesion:	Seabed	1.00 kN/m^2
	Increment (z < 13 m)	0.65 kN/m^2
	Increment (z > 13 m)	1.20 kN/m^2
Interface Strength Reduction		0.65

Only half of the model is used by a symmetric plan cut in the x-y plane. The displacement in the z direction along the symmetric plan boundary is restrained. Lateral limits of each mesh element are held against horizontal displacement, while the basic mesh elements and vertical are held against horizontal displacement. The overall mesh width and length are 15 m and 50 m, respectively. The mesh depths are between 25 m (short pile) and 50 m (long pile). The area surrounding the pile (5 m × 20 m) is modeled with a greater density of 3 times compared to other areas. The total number of elements is about around 8,500 to 11,300 elements. The type of soil elements is 15-node wedge elements, while that of pile walls is 8-node wall elements. Figure 2 shows the typical meshes used in the analysis.

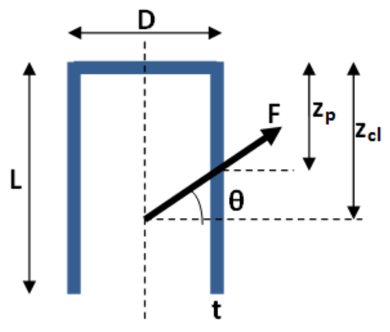

Figure 2 Schematic Drawing of Suction Pile

The schematic drawing of a suction pile and the notations used in this study are shown in Figure 3. The pile diameter used is 5.0 m with aspect ratios L/D of 2 and 6. The load is applied at an angle θ from a horizontal plane. The pad-eye position is at a depth Z_P, while the depth of the intersection of the load line with the pile axis is denoted as Z_{CL}. All cases considered are summarized in Table 2.

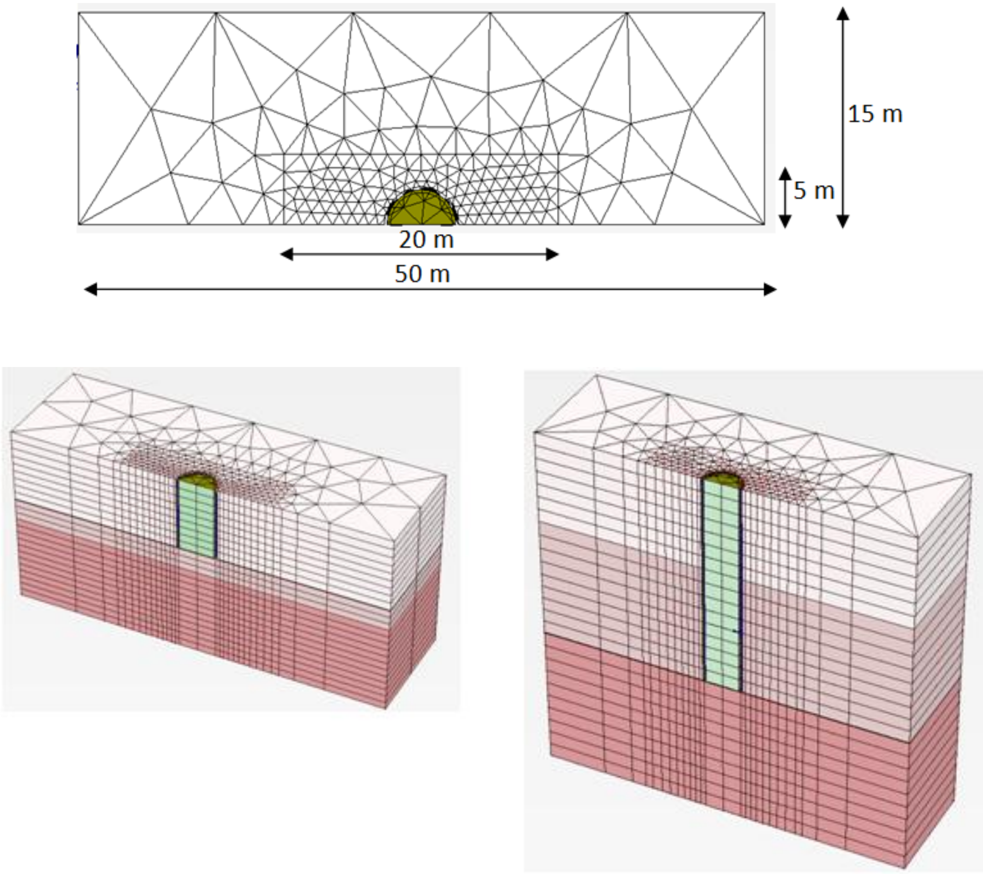

Figure 3 Horizontal Mesh Model and Mesh Element for L/D = 2 and L/D = 6

Table 2 Pile dimension and loading variation

Description	L/D = 2	L/D = 6
Dimension	L = 10.0m, D = 5.0m	L = 30.0m, D = 5.0m
Load angle (Z_{CL} = 0.7 L)	0°, 30°, 45°, 60°, 90°	0°, 30°, 45°, 60°, 90°
Pad-eye position (Load angle = 30°)	Z_{CL} / L = 0.5, 0.7, 0.9	Z_{CL} / L = 0.5, 0.7, 0.9

4. RESULTS AND DISCUSSION

4.1. Effect of Load Angle

The load-displacement curves of L/D = 2 suction piles with different load angles are shown as Figure 4a, while those of L/D = 6 suction piles are shown as Figure 4b. The load angle was relative to a horizontal plane, and the displacement was measured at the pile top centerline. The mooring point Z_{CL} for these cases was 0.7 L. The ultimate resistance of the suction pile was determined as the load at a displacement of 1.5 m. The curves in Figure 4a are within a relatively narrow band, while those in Figure 4b are widely spread. This different behavior is examined further for each suction pile by calculating the ratio of the ultimate resistance to that with a 0° load angle as shown in Figure 5. For L/D = 2 suction piles, the ratio somewhat increases with an increase in load angle, though the ratio subsequently decreases. Furthermore, the horizontal ultimate resistance is not much different from the vertical ultimate resistance. However, for L/D = 6 suction piles, the ratio decreases with an increase in load angle, and the horizontal ultimate resistance is just about half of the vertical ultimate resistance. These results are in agreement with those shown by Supachawarote (2006) for suction piles with different geometry ratio values in normally consolidated clays.

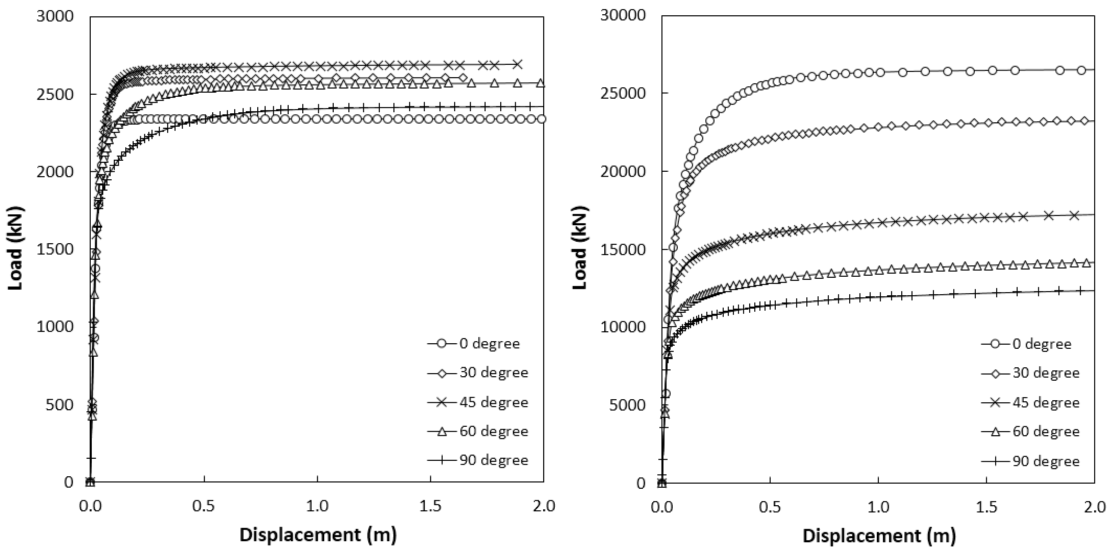

a. L/D = 2 b. L/D = 6

Figure 4 Load-displacement curves suction piles with different geometry

The calculated ultimate resistance is decoupled into the horizontal and vertical resistances for each suction pile. Furthermore, the horizontal resistance is normalized by the ultimate resistance of the suction pile with a 0° load angle, and the vertical resistance is normalized by the ultimate resistance of the pile at a 90° load angle. The results of the decoupling and normalization calculations are as shown in Figure 6.

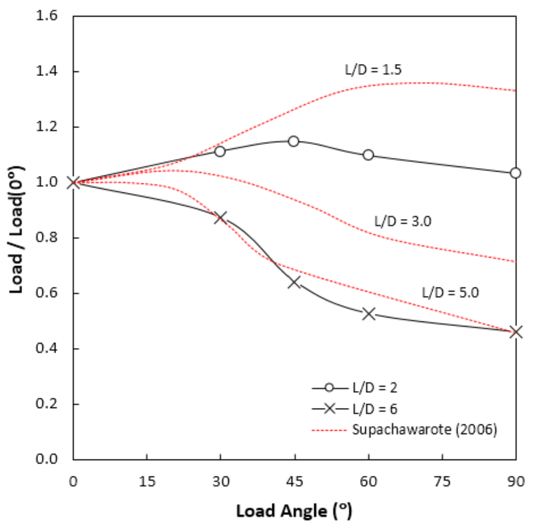

Figure 5 Load ratio vs load angles

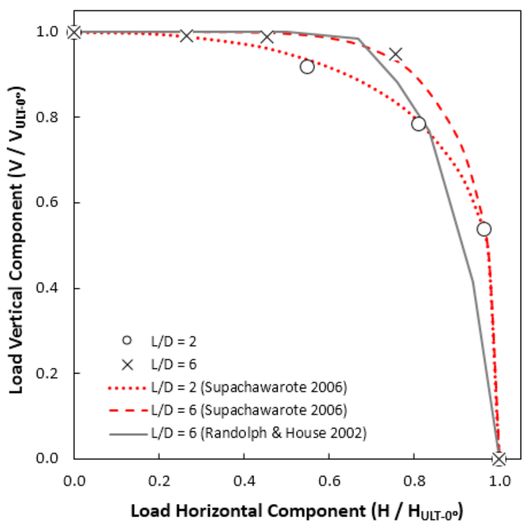

Figure 6 Decoupled resistances

It can be seen that, from this viewpoint, that the aspect ratio does not have a significant effect on the decoupled and normalized results. In addition, for comparison purposes, the horizontal and vertical resistance relationship proposed by Supachawarote (2006) given as Equations 3 through 4 is also shown, and the current study results are practically similar to the proposed envelopes. In addition, the relationship developed from the results of Randolph and House (2002) is also shown for L/D = 6; the current results are comparable to the Randolph and House's results.

The deformation of suction pile and surrounding soil mass for each L/D = 2 suction pile is shown as Figure 7. It is noted that the suction piles are entirely within the under-consolidated soil layer. For low load angles (0° and 30°), the predominant deformation is the horizontal translation. The failure mechanism appears to be in the wedge failure mechanism, as indicated by the settlement of soil on the opposite side of load direction and the bulging of soil on the other side. For higher load angles (60° and 90°), the predominant deformation is in the vertical translation, with an apparent reverse end-bearing failure mechanism. The deformation for each L/D = 6 suction pile is as shown in Figure 8. About a half of the suction piles is within the under-consolidated soil layer, while the other half is within the underlying normally consolidated soil layer. For a load angle of 0°, the predominant deformation is in the horizontal translation, with an apparent wedge failure mechanism. As the load angle increases, the vertical translation appears to become more predominant. It is noted that, for a load angle of 30°, the general deformation pattern for the L/D = 2 suction pile is different from that for the L/D = 6 pile, and this difference could be attributed to the difference in the decoupled horizontal and vertical resistance position shown in Figure 6; for the former, the horizontal resistance ratio is greater than the vertical resistance ratio, indicating the greater relative significance of the horizontal resistance, while for the latter, the vertical resistance ratio conversely is greater than the horizontal resistance ratio. This trend is similar to that observed by Supachawarote (2006).

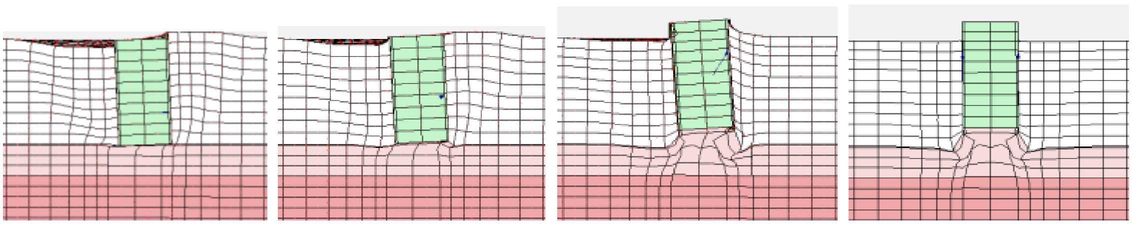

a. Load angle = 0° b. 30° c. 60° d. 90°

Figure 7 Deformation of L/D = 2 suction piles with different load angles

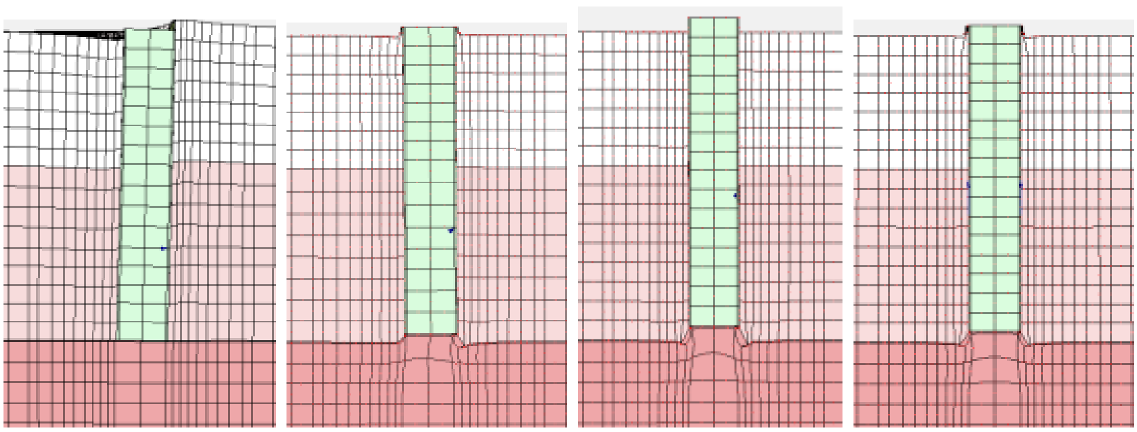

a. Load angle = 0° b. 30° c. 60° d. 90°

Figure 8 Deformation of L/D = 6 suction piles with different load angles

4.2. Effect of Pad-Eye Position

The effect of the pad-eye position, represented by the mooring point Z_{CL}, is also evaluated. Three points are considered, Z_{CL}/L = 0.5, 0.7, and 0.9, while the load angle is maintained at a 30° angle. The resulting resistance is normalized by that for Z_{CL}/L = 0.7 as shown as Figure 9. The ratio trend and magnitude for both L/D = 2 and 6 are practically the same; Z_{CL}/L = 0.7 would be the optimum location, while other Z_{CL}/L values would give a lower resistance. The results are similar to those observed by Supachawarote (2006) for suction piles in normally consolidated and lightly over-consolidated clays.

The deformation of suction pile and surrounding soil mass for each Z_{CL}/L value is shown as Figure 10 for L/D = 2 suction piles and Figure 11 for L/D = 6 suction piles. It can be seen that, for Z_{CL}/L = 0.7, the deformation is a predominantly horizontal translation for L/D = 2 and a predominantly vertical translation for L/D = 6. However, for Z_{CL}/L = 0.5, the predominant pile deformation is clockwise rotational, and the mechanism appears to be a wedge failure mechanism. For Z_{CL}/L = 0.7, the predominant pile deformation is counter-clockwise rotational, and the mechanism appears to be a pile tip spherical rotational flow. It can be concluded that the rotational suction pile deformation appears to be detrimental for the overall pile resistance, with a decrease in resistance in the order of 20 to 30 percent. This trend is similar to that observed by Supachawarote (2006).

4.3. Resistance Factors

The vertical resistance was to determine the reverse end-bearing resistance factor by using Equation 1. Note that the interface adhesion factor is 0.65. The resulting N_H values for L/D = 2 and L/D = 6 suction piles with a 90° load angle are 13.4 and 13.3, respectively. The trend of N_C factor independent of the pile aspect ratio is consistent with that of suction piles in normally consolidated and lightly over-consolidated clays (e.g., Supachawarote 2006).

The horizontal resistance was subsequently used to determine the horizontal resistance factor by using Equation 2. The resulting N_H values for L/D = 2 and L/D = 6 suction piles with a 0° load angle are 11.0 and 12.9, respectively. The trend of increasing N_H values with an increase in the pile aspect ratio is consistent with that of suction piles observed by Supachawarote (2006). It is noted that the resulting N_C and N_H factors appear to be on the upper bounds of the typical respective factors.

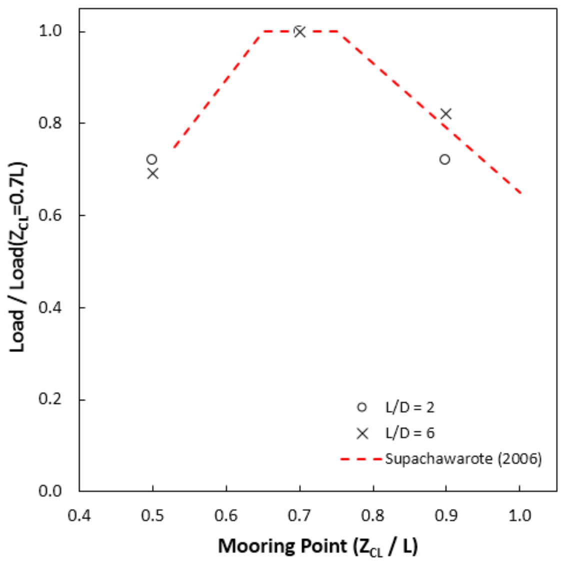

Figure 9 Effect of pad-eye position (load angle = 30°)

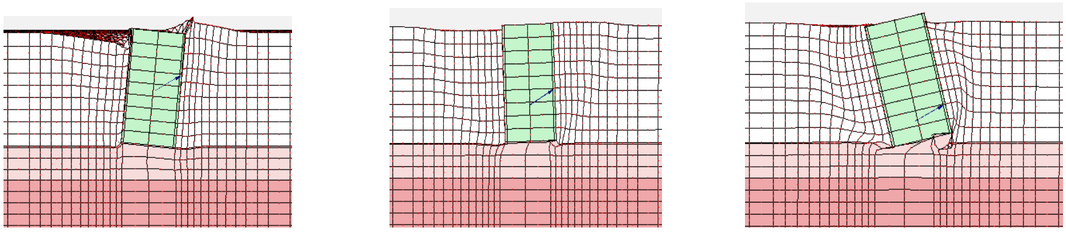

a. Z_{CL} / L = 0.5 b. 0.7 c. 0.9

Figure 10 Deformation of L/D = 2 suction piles with different Z_{CL}

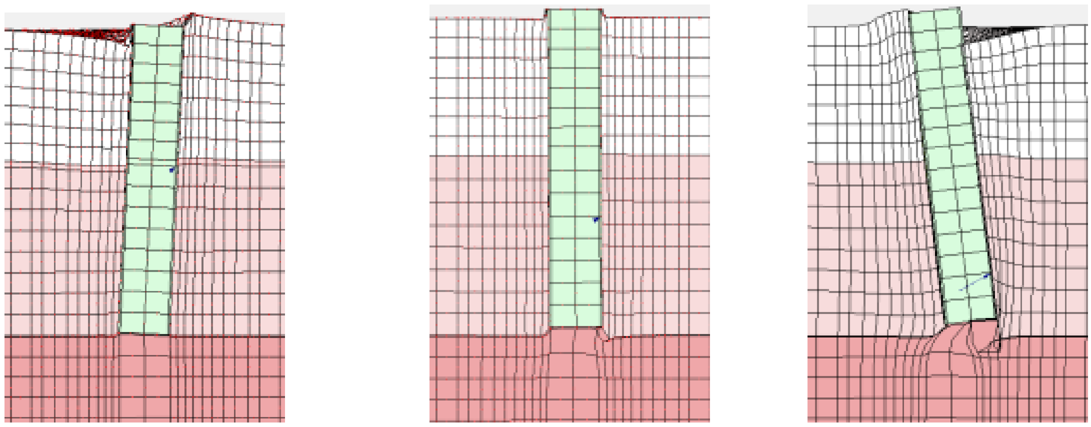

a. Z_{CL} / L = 0.5 b. 0.7 c. 0.9

Figure 11 Deformation of L/D = 6 suction piles with different Z_{CL}

5. CONCLUSION

The behavior of suction piles in under-consolidated clays and under-consolidated, normally consolidated clays was examined using geotechnical 3D finite element models. The current results were compared well to those reported in the literature. These soil conditions were adopted from actual deepwater soil conditions. Suction piles with two different aspect ratios were considered, and the focus was on the effect of load angles and the effects of pad-eye position. For short piles, the load angles had a relatively insignificant effect on the ultimate resistance, while for long piles, the angles affected the resistance considerably. These different behaviors could be explained from the observed pile deformation patterns. The pad-eye positions affected the pile resistances significantly as well. All these results were evaluated against those for suction piles in normally consolidated and lightly over-consolidated clays. The evaluation suggests that the overall behavior of suction piles in combined clay conditions is practically similar to that of piles in normally consolidated and over-consolidated clays.

6. REFERENCES

Andresen, L., Edgers, L., Jostad, H.P., 2008. Capacity Analysis of Suction Anchors in Clay by Plaxis 3D Foundation. *Plaxis Bulletin*, Issue 24, October, pp.5–9

Dutt & Associates Inc., 2007. Interpretive Report on Soil Conditions Gehem and Ranggas Prospects Offshore East Kalimantan, Indonesia. (unpublished report)

Plaxis B.V., 2008. *Plaxis 3D Foundation, version 2.1*. Delft, the Netherland

Randolph, M.F, House, A.R., 2002. Analysis of Suction Caisson Capacity in Clay. *Proceedings of the 2002 Offshore Technology Conference*, Houston – Texas USA, 6-9 May 2002

Supachawarote, C., 2006. Inclined Load Capacity of Suction Caisson in Clay, *PhD Thesis*, School of Civil and Resource Engineering, The University of Western Australia, p. 164